International Journal of Mechanical, Industrial and Aerospace Sciences
ISSN: 2517-9950
Vol:2, No:4, 2008

Effect of Particle Gravity on the Fractal Dimension of Particle Line in three-dimensional Turbulent Flows using Kinematic Simulation

A. Abou El-Azm Aly, F. Nicolleau, T. M. Michelitsch, and A. F. Nowakowski

Abstract**—**In this study, the dispersion of heavy particles line in an isotropic and incompressible three-dimensional turbulent flow has been studied using the Kinematic Simulation techniques to find out the evolution of the line fractal dimension. The fractal dimension of the line is found in the case of different particle gravity (in practice, different values of particle drift velocity) in the presence of small particle inertia with a comparison with that obtained in the diffusion case of material line at the same Reynolds number. It can be concluded for the dispersion of heavy particles line in turbulent flow that the particle gravity affect the fractal dimension of the line for different particle gravity velocities in the range $0.2 < W < 2$. With the increase of the particle drift velocity, the fractal dimension of the line decreases which may be explained as the particles pass many scales in their journey in the direction of the gravity and the particles trajectories do not affect by these scales at high particle drift velocities.

Keywords**—**Heavy particles, two-phase flow, Kinematic Simulation, Fractal dimension.

I. Introduction

TURBULENT flows consist of eddies of different sizes which affect the shape of a line immersed in them. Finding the geometry of this line, which may represent the boundary between two mixing fluids in a combustion process for example, is expected to put some lights on the turbulence flow analysis and explains some behavior of objects immersed in that flow and because of the fine structure of this line it can be presented by using the fractal geometry concept. Also understanding the fractal dimension of heavy particle lines is important for accurate modeling of the scalar mixing and the flamelet propagation aspects of combustion.

Most of the previous studies have been done for fluid element particles, in which the fractal dimension of a material line has been found either experimentally or using simulation methods. In [1], they investigated experimentally the time evolution of an initially regular passive dye in three-dimensional homogeneous turbulence in a line-dispersion. They also derived an expression for the fractal dimension of a line immersed in homogeneous turbulence that compares very well with the experiment at different Reynolds numbers. This expression relates the fractal dimension to time and Reynolds number:

$$D = 1 + 0.088\left(\frac{t}{t_d}\right) Re^{1/2} \quad (1)$$

where D is the fractal dimension of the line, t_d is the turnover time, the Reynolds number $Re=(L/\eta)^{4/3}$, ε is the dissipation rate per unit mass, L is the integral length scale and u` is the rms value of the turbulence fluctuation. The fractal dimension was found to increase linearly with time at a rate increasing with the increase in the Reynolds number. In [2] they studied the fractal dimension of a line embedded in a homogenous turbulent flow using a Large Eddy Simulation. It is shown that the fractal dimension of the line increases with time. The simulation results were compared to experiments and theory developed by [1]. But this was only validated on a limited range of Reynolds numbers. However in [3], they studied the development of the fractal dimension of material lines formed from the fluid elements immersed in turbulent flows using kinematic simulation which able them to produce high Reynolds numbers and simulate the small scales of the turbulence. They validated the equation in [1] for the obtained results from kinematic simulation; they found that the fractal dimension of a line is a linear relation of time up to times of the smallest scale of turbulence.

The numerical method we use to generate the turbulent flow is introduced in II, fractal dimension calculation method is outlined in II and the heavy particle equation of motion is introduced in III. The simulation parameters used are presented in IV and the results for the fractal dimension of line immersed in turbulent flow are presented in V. We conclude the paper in VI.

II. Kinematic Simulation

Kinematic Simulation provides the Lagrangian model of turbulent dispersion based on a simplified incompressible velocity field, where the incompressibility is enforced by construction in the generation of every particle trajectory, kinematically simulated the Eulerian velocity field which is

A. Abou El-Azm Aly is a PhD student in the Department of Mechanical Engineering, The University of Sheffield, Mappin Street, Sheffield, UK, S1 3JD (e-mail: .A.Aboazm@Sheffield.ac.uk).

F. Nicolleau is a senior lecturer in the Department of Mechanical Engineering, The University of Sheffield, Mappin Street, Sheffield, UK, S1 3JD (e-mail: F.Nicolleau@Sheffield.ac.uk).

T. M. Michelitsch is a senior lecturer in CNRS UMR 7190, Institut Jean le Rond d'Alembert, Paris, France (e-mail: michel@lmm.jussieu.fr).

A. F. Nowakowski is a lecturer in the Department of Mechanical Engineering, The University of Sheffield, Mappin Street, Sheffield, UK, S1 3JD (e-mail: A.F.Nowakowski@Sheffield.ac.uk).

generated as a sum of random incompressible Fourier modes with a proper wavenumber-energy spectrum which has the Kolmogorov form.

As in [4]-[6] the three-dimensional KS turbulent velocity field used in this paper is a truncated Fourier series, the sum of N random Fourier modes:

$$u_E(x(t),t)=\sum_{n=1}^{N_k}\left[\left(\vec{a}_n\times\hat{k}_n\right)\cos(\vec{k}_n\cdot x+\omega_n t)+\left(\vec{b}_n\times\hat{k}_n\right)\sin(\vec{k}_n\cdot x+\omega_n t)\right] \quad (2)$$

where N_k is the number of Fourier mode, $\hat{k}_n$ is a random vector distributed independently and uniformly over a unit sphere $\vec{k}_n=k_n\hat{k}_n$ and $\vec{a}_n$ and $\vec{b}_n$ are chosen randomly vectors under certain constrains that they are normal to $\hat{k}_n$. $|k_n|$ is the modulus of the wavenumber k_n so that :

$$\vec{k}_n=|k_n|\begin{pmatrix}\sin\theta_n\cos\phi_n\\ \sin\theta_n\sin\phi_n\\ \cos\theta_n\end{pmatrix} \quad (3)$$

where $\theta_n\in[0,\pi]$ and $\phi_n\in[0,2\pi[$ are picked randomly in each mode and realization so that the random choice of directions for the n^{th} wavemode is independent of the random choice of directions for all others. The $\vec{a}$ and $\vec{b}$ vectors in Eq. (2) are random and uncorrelated vectors orthogonal to k_n vector with their amplitude being chosen according to:

$$|A_n|^2=|B_n|^2=2E(k)dk \quad (4)$$

and to ensure that the velocity field is incompressible ($\nabla.u=0$), the Fourier coefficients are written as $\left(\vec{a}_n\times\hat{k}_n\right)$ and $\left(\vec{b}_n\times\hat{k}_n\right)$. The discretization of the wavenumber can be achieved by one of the following distributions:

$$k_n=k_1\left(\frac{k_\eta}{k_1}\right)^{n-1/N_k-1} \quad (5)$$

because the geometric distribution leads to equally spaced energy shells for log(k). It has been shown that when the energy spectrum input has the kolmogorov (-5/3) form, in this study we will use an energy spectrum, E(k), which does not change with time (non-decaying turbulence) has the following form:

$$E(k)=\begin{cases}C_k\varepsilon^{2/3}k^{-5/3} & k_1<k<k_\eta\\ 0 & \text{otherwise}\end{cases} \quad (6)$$

Then the turbulent velocity fluctuation intensity is:

$$u'=\sqrt{\frac{2}{3}\int_{k_1}^{k_N}E(k)dk} \quad (7)$$

The following definition of the integral length scale of the isotropic turbulence has been used:

$$L=\frac{3\pi}{4}\frac{\int_{k_1}^{k_N}k^{-1}E(k)dk}{\int_{k_1}^{k_N}E(k)dk} \quad (8)$$

The ratio between the integral length scale to Kolmogorov length scale is $\frac{L_1}{\eta}=\frac{k_N}{k_1}$ and determined the inertial range and the associated Reynolds number which is related to the inertial range is

$$\mathrm{Re}\approx\left(\frac{L_1}{\eta}\right)^{4/3}\approx\left(\frac{k_N}{k_1}\right)^{4/3} \quad (9)$$

It is also possible to introduce a frequency ω_n that determines the unsteadiness associated with the nth wavemode. This parameter enables us to create 3-D effects in the case of a 2-D simulation, to mix up the velocity field and to improve the turbulence. In the 3-D KS field, the previous studies suggest that the choice of ω_n has no significant influence on most statistical properties of two particle diffusion for time less than the integral time scale T_L. The frequency ω_n is proportional to the eddy-turn-over frequency of mode n, and the dimensionless constant of proportionality is λ. It has been shown in [7] that in three-dimensional isotropic KS for two-particle diffusion, most of the statistical properties are insensitive to the unsteadiness parameter's value, provided that it rests in the range $0<\lambda<1$. In accordance with these results we have not added any unsteadiness term ($\lambda=0$) to our KS simulations. One of the most important characteristic times in the turbulent flow is the eddy turn over time scale which corresponds to the integral length scale and the other is the Kolmogorov time scale which corresponds to the Kolmogorov length scale. The eddy turnover time is the time needed for the largest eddy to turn around itself and defined as

$$t_d=\frac{L}{u'} \quad (10)$$

Before the eddy turnover time, the particle remembers its initial position, while after this time, the particles are free to move randomly. The Kolmogorov time scale is the time needed for a particle to move a distance η when its velocity equal to v_η and is defined as follows:

$$t_\eta=\frac{\eta}{v_\eta} \quad (11)$$

According to [8], a time step equal to 0.1 t_η is small enough to ensure that the results are independent of the time step. This technique, KS, has been able to reproduce very well some of the Lagrangian properties [7], [9]. The computational simplicity of KS allows one to consider large inertial sub-ranges and Reynolds numbers. With this method, the computational task reduces to the calculation of the trajectory of each particle placed in the turbulent field; each trajectory is, for a given initial condition, solution of the differential equation:

$$\frac{dx(t)}{dt}=u_E(x(t),t) \quad (12)$$

where u_E is the Eulerian velocity field which is chosen as a sum of Fourier modes as in Eq. 2). The trajectories are independent of each other and calculated using the 4^{th} order predictor-corrector method (Adams-Bashforth-Moulton) in which Runge-Kutta-4 is used to compute the first three points needed to initiate Adams-Bashforth's method. This kind of

computation does not require the storage of a lot of data with very large tables as with direct numerical simulation.

III. Heavy Particle Equation of Motion

The equation of motion for heavy particles is still the subject of current research. Depending on the degree of simplification, it can involve different forces acting on the particle. These forces are due to the relative motion between the particle itself and the surrounding fluid elements. Let's consider a heavy particle with its centre positioned at $x_p(t)$ at time t moves with a velocity v(t) in the surrounding flow field of velocity $u(x_p,t)$. The equation of motion of a heavy sphere particle can be calculated as:

$$m_p \frac{dV_p}{dt} = \sum F_{acting}(u(x_p, t), V_p, t) \quad (13)$$

where the RHS of Eq. 13 is the sum of all forces acting on the particle. With some simplifications; the mass density of the heavy particle is assumed to be much heavier than the surrounding fluid density the radius of the heavy particle sphere is assumed to be smaller than the smallest length scale of the turbulence the Kolmogorov length scale of turbulence then the heavy particle will respond to all scales of the turbulent flow and will not affect the turbulence itself, also as the radius of the heavy particle sphere is considered to be much larger than the fluid molecules free path then the particle aerodynamic response time much larger than the mean molecular collision time and there is no Brownian motion effect, the Reynolds number based on it being much smaller than unity then one can consider the drag force on the heavy particle as Stockesian drag, finally, the concentration of particles in the fluid flow field must be small enough to make sure that the interaction between the particles could be ignored, the equation of motion of a heavy particle derived in [10] can be simplified to the form used in [11]-[12], which reduces the computational cost. In a frame of reference moving with the center of the particle, the particle acceleration can be described as follows:

$$m_p \frac{dv}{dt} = m_p g - 6\pi a\mu(v - u) \quad (14)$$

where m_p is the mass of the particle, g is the gravity, a is the spherical particle's radius and μ is the dynamic viscosity of the fluid, another form of Eq. 14 is:

$$\frac{dv}{dt} = \frac{u - v + V_d}{\tau_a} \quad (15)$$

where $\tau_a = m_p/6\pi a\mu$ is the particle's aerodynamic response time and $V_d = \tau_a g$ is the particle's terminal fall velocity or drift velocity. Because the dispersion is controlled by the large scale eddies, the parameters V_d and τ_a can be rescaled by the turbulence rms velocity, u', and the largest eddy turnover time, t_d, we therefore introduce the two usual dimensionless parameters: the Stokes number, $St = \tau_a / t_d$, which expresses the ratio between the particle's response time and the turbulence characteristic time. The drift velocity parameter, $W=V_d / u'$, which is the ratio between the particle's drift velocity and the turbulence rms velocity.

IV. Fractal Dimension Calculation

Fractal geometry does not replace the classical geometry but enriches and deepens it, high performance computers allow one to build fractal shapes and calculate their fractal dimension. The modified box counting method (MBCM) is used here because it is the most popular way of estimating the fractal dimension because of its simplicity. This method was refined over the years to simplify the Hausdorff dimension, in the box-counting method, the fractal object is covered with a network of boxes and its principle is based on the fact that the number of boxes (N_ε) having a side length (ε) needed to cover the surface of this fractal object varies as ε^{-D}, where D is the estimation of the fractal dimension of the object under study, as in Fig. 1.

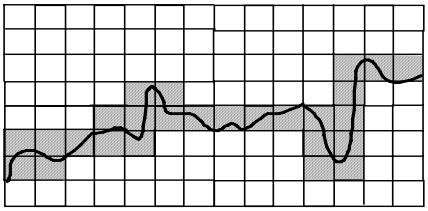

Fig. 1 Box Counting method

While the magnitude of the box side is changed in each step this number of boxes (N_ε), necessary for this coverage of the object perimeter, is detected. The relation between the number of boxes and the magnitude of the box side determines the value of the fractal dimension D as follows:

$$D = \frac{\log N_\varepsilon}{\log(1/\varepsilon)} \quad (16)$$

using this formula and by recoding the number of boxes with the box side, one is able to find the fractal dimension of the heavy particle line after a certain time step by computing the slope of Equation 16.

V. Simulation Parameters for the Heavy Particles Line

For each of our simulations, the particle equation of motion Equation 14 was integrated over 4000 realizations of the flow the initial velocity of the heavy particle is set to be the same as that of the fluid element. All simulations reported here were performed using two hundred Fourier modes (N=200). The particle drift velocities are set to be 0.2, 1 and 2 at St=0.02 in addition to the case of material line diffusion. Runs have been made for k_N/k_1=36, 100, 178 and 1000, the fractal dimension is calculated as a function of the time evolution. The studied line is released in a horizontal plane where z = -0.25L and from point (-2.5L, 2.5L) to point (2.5L, 2.5L).

VI. Results

The fractal dimension was calculated for different values of particles inertia to investigate its significance in the dispersion of heavy particles line. The fractal dimension of the heavy particle line was calculated at different time steps.

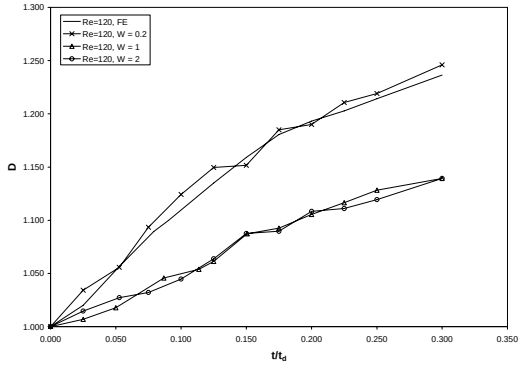

Fig. 2 Fractal dimension of heavy particle lines as a function of the normalized for k_N/k_1=36 and different particle drift velocities

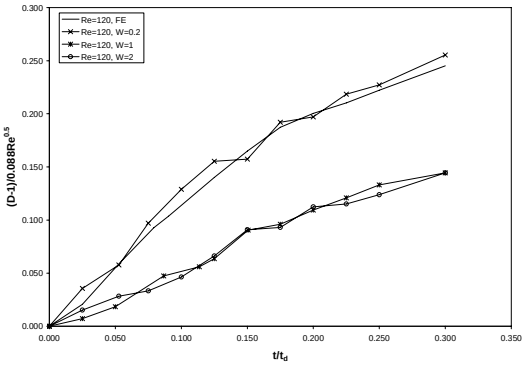

Fig. 3 Normalized fractal dimension of heavy particle lines as a function of the normalized time for k_N/k_1=36 and different particle drift velocities

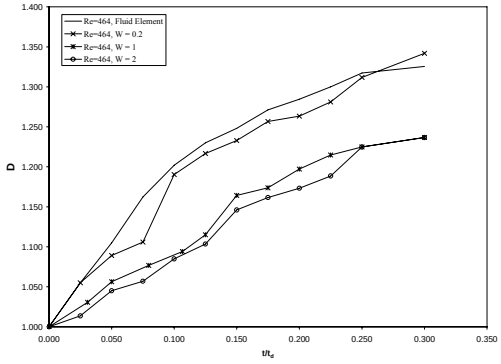

Fig. 4 Fractal dimension of heavy particle lines as a function of the normalized time for k_N/k_1=100 and different particle drift velocities

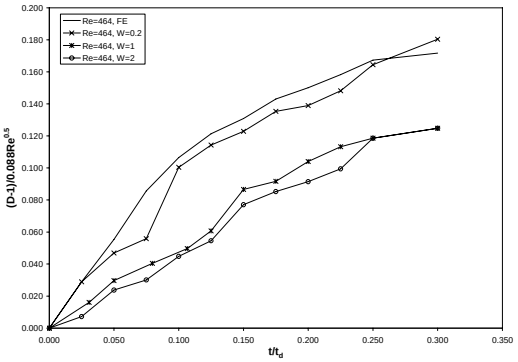

Fig. 5 Normalized fractal dimension of heavy particle lines as a function of the normalized time for k_N/k_1=100 and different particle drift velocities

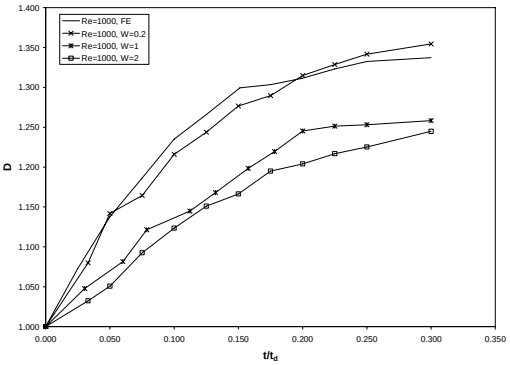

Fig. 6 Fractal dimension of heavy particle lines as a function of the normalized time for k_N/k_1=178 and different particle drift velocities

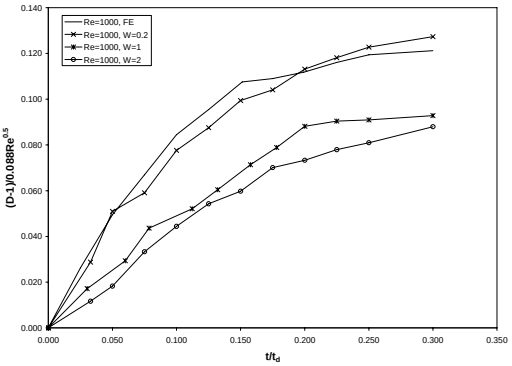

Fig. 7 Normalized fractal dimension of heavy particle lines as a function of the normalized time for k_N/k_1=178 and different particle drift velocities

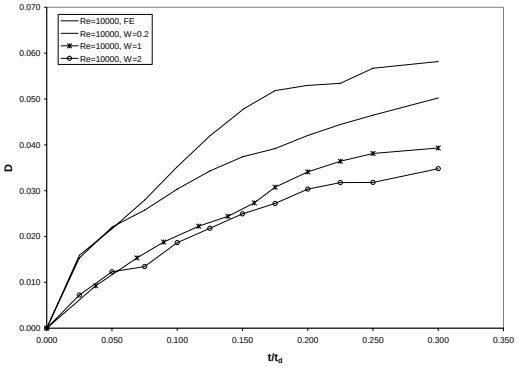

Fig. 8 Fractal dimension of heavy particle lines as a function of the normalized time for k_N/k_1=1000 and different particle drift velocities

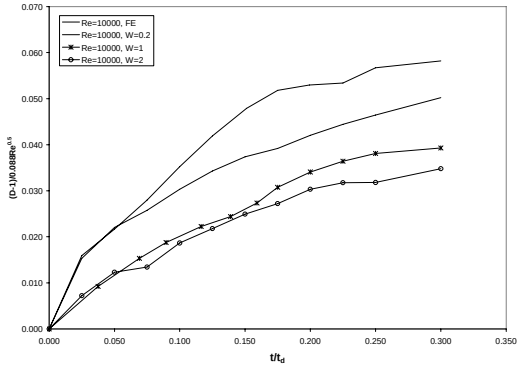

Fig. 9 Normalized fractal dimension of heavy particle lines as a function of the normalized time for k_N/k_1=1000 and for different particle drift velocities

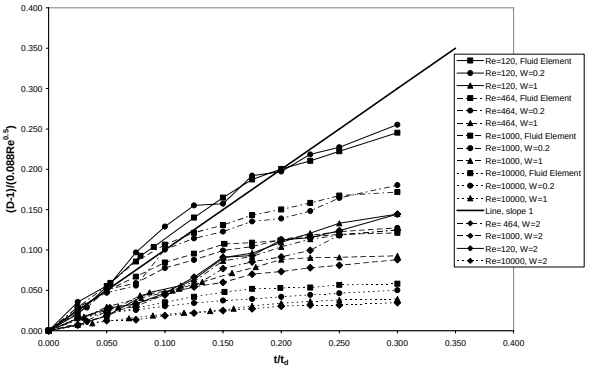

Fig. 10 Normalized fractal dimension of heavy particle lines as a function of the normalized time for different k_N/k_1, different particle drift velocities and the slope of line 1

REFERENCES

[1] E. Villermaux and Y. Gagne, Physical Review Letters, Vol. 73, No. 2, pp. 252, 1994.
[2] F. Nicolleau, Phys. Fluids, Vol. 8, No. 10, pp. 2661, 1996.
[3] F. Nicolleau and A. ElMaihy, J. Fluid Mech., Vol. 517, pp. 229, 2003.
[4] P. Flohr and J. C. Vassilicos, J. Fluid Mech., Vol. 407, pp. 315, 2000.
[5] A. ElMaihy and F. Nicolleau, Phys. Rev. E 71, pp. 046307, 2005.
[6] F. Nicolleau and A. ElMaihy, Phys Rev. E 74, pp. 046302, 2006.
[7] N. A. Malik and J. C. Vassilicos, Phys. Fluids 11, pp. 1572, 1999.
[8] J. C. H. Fung, Ph.D. thesis, University of Cambridge, 1990.
[9] F. Nicolleau and J.C.Vassilicos, Physical Review Letters, Vol. 90, pp. 024503, 2003.
[10] M. R. Maxey and J. J. Riley, Physics of Fluids 26, pp. 883, 1983.
[11] M. R. Maxey and L.-P. Wang, Experimental Thermal and Fluid Science Vol. 12, pp. 417, 1996.
[12] M. R. Maxey and L.-P. Wang, Fluid Dynamics Research 20, pp. 143, 1997.